Application of coarse gibbsite agglomerates to formation of 2D and 3D boehmite particles by the dehydration of the hydrothermal treatment and atmospheric pressure

Svetlana R. Egorova[a],*, Zhang Yuqing[a,b], Aliya N. Mukhamed'yarova[a], Asiya Z. Kurbangaleeva[a], Alexander A. Lamberov[a]

[a] Alexander Butlerov Institute of Chemistry, Kazan Federal University, Kazan, st. Kremlevskaya, 29/1, 420008, Russian Federation.
[b] Institute of Chemistry, Chemical Engineering and Materials, Heilongjiang University, Harbin, st. Xuefu, 74,150080, China

A B S T R A C T

The coarse agglomerates of gibbsite (γ-Al(OH)$_3$) are grateful starting materials for preparation aluminum oxides and hydroxides as boehmite and γ-Al$_2$O$_3$, which are extensively used as a catalysts and catalyst support for the petrochemical industry. By preparing the boehmite particles from the gibbsite and product of the heat gibbsite, we demonstrate the influence of different treatments to a morphology and particle size of the formed boehmite (γ-AlOOH). It is been established for the first time that the flaky-shaped 2D γ-AlOOH particles are formed within the coarse agglomerates producing a laminated packaging film lozenge-shaped crystals which results in a 0.1 cm^3/g pore volume and 29 m^2/g specific surface area. The obtained data have a high industrial importance in the area of producing materials based on the coarse boehmite agglomerates with different properties.

1. Introduction

Gibbsite (γ-Al(OH)$_3$) is known to be the cheapest and significant raw materials of alumina–ceramic. γ-Al(OH)$_3$ is a very popular engineering product produced by Bayer method on an industrial scale. Boehmite (γ-AlOOH) can also be synthesized by the direct hydrothermal treatment of gibbsite under the temperature of 120–380 °C at the appropriate saturated vapor pressure of water. In recent years, γ-AlOOH particles with nanoscale dimentions and morphological specificity have attracted enormous interest from both fundamental and practical viewpoints [1–13]. Additionally, γ-AlOOH is one of the most important hydroxides because of their potential for broad applications in petrochemical refining process, advanced catalysis, adsorption, composite materials design and ceramics [1–8]. Boehmite is also used as a flame retardant in plastics and paint materials, as a component of the toothpastes, an enveloping and absorbing material in medicine. Under heat treatment of more than 1000 °C γ-AlOOH turns into corundum which is used in industry as a catalyst support for a partial oxidation in the production of ceramics and constructional materials, abrasives, also in the laser technology and microelectronics. Boehmite is widely used in industry as a precursor of alumina. γ-AlOOH is transformed to γ-Al$_2$O$_3$ under heat treatment of 350–750 °C. The alumina is also the most commonly used support material in traditional

catalysts designed to remove NO$_x$ from auto exhausts [9]. The alumina is the porous support for the supported ionic liquids phase where ionic liquids is an alternative solvent in a range of catalytic processes as compared to traditional volatile organic solvents for developing greener reactions [10].

Generally, specific properties of the most important aluminum oxides based materials (catalysts, catalyst supports, adsorbents and ceramics) such as a specific surface area, pore volume, shape, size and the granules strength depend largely on the structural characteristics of its precursor (its size, morphology and character packing arrangement of boehmite particles). For example, when γ-AlOOH crystallizes at the deterioration of amorphous aluminum hydroxide at atmospheric pressure or under hydrothermal conditions boehmite particles can be shaped in the form of nanospheres [1], hollow microspheres or microelipsoids [2,3] nanowires [4], the flowers [5], flat sheets [6], nanorods [7] and nanotubes [8] which depend on the synthesis conditions. Mesoporous clusters of spherical boehmite microparticles are obtained by hydrolysis of aluminum metal [11]. To develop a simple synthesis route for the control over the morphology of AlOOH is of great importance for broadening and improving their industrial applications. For example, γ-AlOOH particles in the form of sword [12], in the shape of plates [13] and parallelepipeds [14] were synthesized by the autoclave treatment of γ-Al(OH)$_3$. In the work mentioned above the

authors used γ-Al(OH)$_3$ particles with the very small sizes (1.5–50 μm) which were obtained by grinding or screening of the fraction. However, much larger aggregates of γ-Al(OH)$_3$ crystals (agglomerates) are produced by the Bayer method which is almost spherical with a diameter of more than 200 microns in [15]. These large agglomerates are used as precursors of microsphere catalysts support. Therefore, the studying of the influence of the hydrothermal treatment conditions of γ-Al(OH)$_3$ large agglomerates on the morphological features of crystallizing γ-AlOOH particles and their sizes is of a large scientific and practical importance. The synthesis of flaky-shaped 2D γ-AlOOH particles formed within the coarse agglomerates producing a laminated packaging film lozenge-shaped crystals which results in a 0.1 cm^3/g pore volume and 29 m^2/g specific surface area have not been reported so far. The aim of this paper is to present the results of different morphology (parallelepipeds, plates and flakes) boehmite particles synthesis in the hydrothermal treatment of gibbsite agglomerates (40–180 μm) under the "dry" steam or an aqueous suspension with and without using intermediate heat treatment.

2. Material and methods

2.1. Equipment and materials

Gibbsite (γ-Al(OH)$_3$) produced by ETI ALYMINUM A.S. (Turkey) is used for the synthesis of boehmite. According to the passport data, the concentration of Na$_2$O in gibbsite is 0.15 wt%. The agglomerates (40–180 μm) were obtained by sieving the gibbsite powder (Fig. 1 (curve 1)).

The hydrothermal treatment was performed by a BüchiGlasUster 'Limbo li' autoclave with automated temperature and pressure control in a 450 mL stainless steel reactor with an alumina to water mass ratio of 1:5 and with an agitation by a stirrer at speed of 500 rpm and the maximum autoclave filling of 70%. The X-ray diffraction (XRD) method on a Shimadzu XRD-7000 advance diffractometer with Cu Kα radiation (λ = 1.5406 Å) was used to study the phase of the samples. The phase concentrations were obtained using the thermal analysis (TA; Netzsch STA–449C Jupiter analyser coupled with a QMS 403 Aeolos quadrupole mass-spectrometer). The measurements by scanning electron microscopy (SEM) were carried out with an EVO 50XVP electron microscope combined with an INCA 350 energy-dispersive spectrometer.

The specific surface area S$_{BET}$ (S$_{BET}$ – a specific surface area calculated with the Brunauer—Emmett—Teller method) and the pore volume V$_{BET}$ (V$_{BET}$ – a pore volume calculated with the Brunauer−Emmett−Teller method) were determined using a multipurpose Quantachrome Autosorb iQ analyser. The particle size distribution was determined by the laser microprobe of particles «Mastersizer 2000» (Malvern Instruments Ltd, UK). Analysis of samples

was carried out in a transmission electron microscope (TEM) Hitachi HT7700 Excellence. ^{27}Al NMR spectra were recorded with an Avance II 500 spectrometer at the frequency of 130.32 MHz. The samples were a mixture of the investigated solutions in an amount of 550 μL with addition of 50 μL of D$_2$O.

2.2. Procedures and samples

In this article we investigated following samples: S1 - the product of γ-Al(OH)$_3$ hydrothermal treatment under the "dry" steam (without de-ionized water); S2 - the product of γ-Al(OH)$_3$ hydrothermal treatment in an aqueous suspension; S3 - the product of the γ-Al(OH)$_3$ heat treatment; S4 - the product of the γ-Al(OH)$_3$ heat treatment hydrothermal treatment in an aqueous suspension (treatment conditions shown on the Table 1).

The heat treatment of γ-Al(OH)$_3$ agglomerates was performed by a muffle furnace at 350 °C for 180 min. The hydrothermal treatment in the aqueous suspension was conducted with the weight ratio γ-Al(OH)$_3$/heating product: de-ionized water = of 1:5. The pH value of the starting aqueous suspension of γ-Al(OH)$_3$ and heating product are 10.5 and 9.5, respectively. The temperature increase in autoclave was carried out for approximately 60 min until the required temperature was reached. The autoclave reactor was cooled by feeding its jacket with the cold water. As a result, its temperature was decreased to 100 °C in 20 min.

3. Calculation

The sizes of coherent scattering regions (CSR) $D_{(hkl)}$ were calculated using the Scherrer equation:

$$D_{(hkl)} = K \times \lambda/(\beta \cdot cos\theta).$$

The equation limited by the uncertainties in K, the crystallite shape factor, and β, which is the pure diffraction broadening. Diffraction intensities were measured by varying the angle from 10 to 80° (2θ) with a step size of 0.02° (2θ). The phase identification was done according to the presence of the following diffraction lines in the X-ray spectrum: γ-Al(OH)$_3$ (JCPDS Card 01-076-3811), γ-AlOOH (JCPDS Card 00-021-1307), χ-Al$_2$O$_3$ (JCPDS Card 00-013-0373).

4. Results and discussion

X-ray pattern of γ-Al(OH)$_3$ is shown on Fig. 2(a) and it is typical for an aluminum hydroxide.

According to SEM the γ-Al(OH)$_3$ are the round-shaped crystalline aggregates composed of the block particles of the size less than10 μm with a hexagonal profile (Fig. 3a).
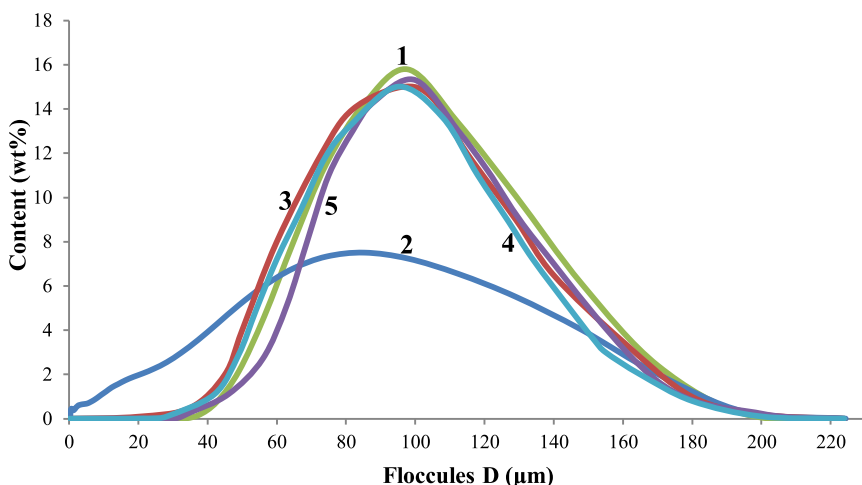

Fig. 1. Distribution curves of agglomerates diameters: **1** – γ-Al(OH)$_3$; **2** – the product of γ-Al(OH)$_3$ hydrothermal treatment under the "dry" steam; **3** – the product of γ-Al(OH)$_3$ hydrothermal treatment in an aqueous suspension; **4** – the product of heat treatment of γ-Al(OH)$_3$; **5** – the hydrothermal treatment in an aqueous suspension product of the heat treatment sample.

Table 1
Characteristics of γ-Al(OH)$_3$ and its hydrothermal and heat treatment products.

Precursor	Hydrothermal treatment conditions					Phase	C(Bm), wt/%	Boehmite CSR size, nm		Porous system parameters		
	envi-romen-tal	T, °C	P, MPa	τ, min	pH			$D_{(020)}$, nm	$D_{(120)}$, nm	S_{BET}, m^2/g	V_{BET}, cm^3/g	D_p, nm
γ-Al(OH)$_3$	initial					γ-Al(OH)$_3$	–	–	–	0.1	0.007	4.5
	"dry" steam	200	1.6	300	–	γ-AlOOH	100	38.1	39.0	2.6	0.009	11.3
	H$_2$O	200	1.7	60	10.5	γ-AlOOH	100	70.2	55.3	1.3	0.003	2.9
The sample S3	initial					γ-AlOOH, χ-Al$_2$O$_3$	63	38.3	33.3	223.0	0.200	3.5
	H$_2$O	200	1.7	60	9.5	γ-AlOOH, χ-Al$_2$O$_3$	99	51.5	43.0	29.0	0.100	13.0

According to the Table 1, γ-Al(OH)$_3$ has a nonporous structure. The pores are just the cracks in its crystals (Fig. 3b). The phase composition of the hydrothermal and heat treatments of γ-Al(OH)$_3$ products, the coherent scattering regions' (CSR) sizes and sample parameters of the porous system are given in Table 1. When the pressure in the autoclave in a confined space is created only by the water vapor given out during γ-Al(OH)$_3$ dehydration in a "dry steam" environment the total phase transition into γ-AlOOH takes 300 min (Fig. 2b). On the differential scanning calorimetry (DSC) curve of the obtained sample we can see an endothermic effect within a temperature minimum of the dehydration of γ-AlOOH to γ-Al$_2$O$_3$ at 520 °C. The process is accompanied by dispersion of the agglomerates. The large number of smaller particles can be seen in the sample obtained by autoclaving (Fig. 1, curve 2). The number of particles of the original size is reduced almost third while the rest of the particles have a diameter of 0.3–40 μm (Fig. 3d). The dispersion is caused by intensive release of water into the gaseous medium with the dehydration of gibbsite to boehmite.

Thus, as it is shown on the Fig. 3c, d, the lamellar, rectangle-shaped 2D particles are formed primarily. We can supposed that under the "dry steam" conditions during the dehydration the part of γ-Al(OH)$_3$ crystals are stratified into plates along the (001) plane. As a result, the known processes of γ-Al(OH)$_3$ particles dissolution, aluminum complexes deposition, nucleation and subsequent growth of 2D γ-AlOOH particles happen within those plates due to the small amounts of the water molecules released. The specific surface area, pore volume and average pore diameter of the sample are increased in comparison with γ-Al(OH)$_3$ as a consequence of 2D γ-AlOOH particles formation (Table 1).

Unlike the case of "dry steam" during the hydrothermal treatment of γ-Al(OH)$_3$ in an aqueous suspension (pH = 10.5, a purification of the aqueous solution part of sodium ions) the agglomerates are not dispersed (Fig. 1, curve 3). They are partially cracked as is shown on the Fig. 3e. γ-Al(OH)$_3$ is fully dehydrated to γ-AlOOH in 60 min (Fig. 2c). According to the SEM (Fig. 3f), γ-AlOOH 3D particles, which have the form of parallelepipeds and lozenges with edge to 2 μm, are crystallized inside cracked agglomerates. In that case the minimum sizes of the
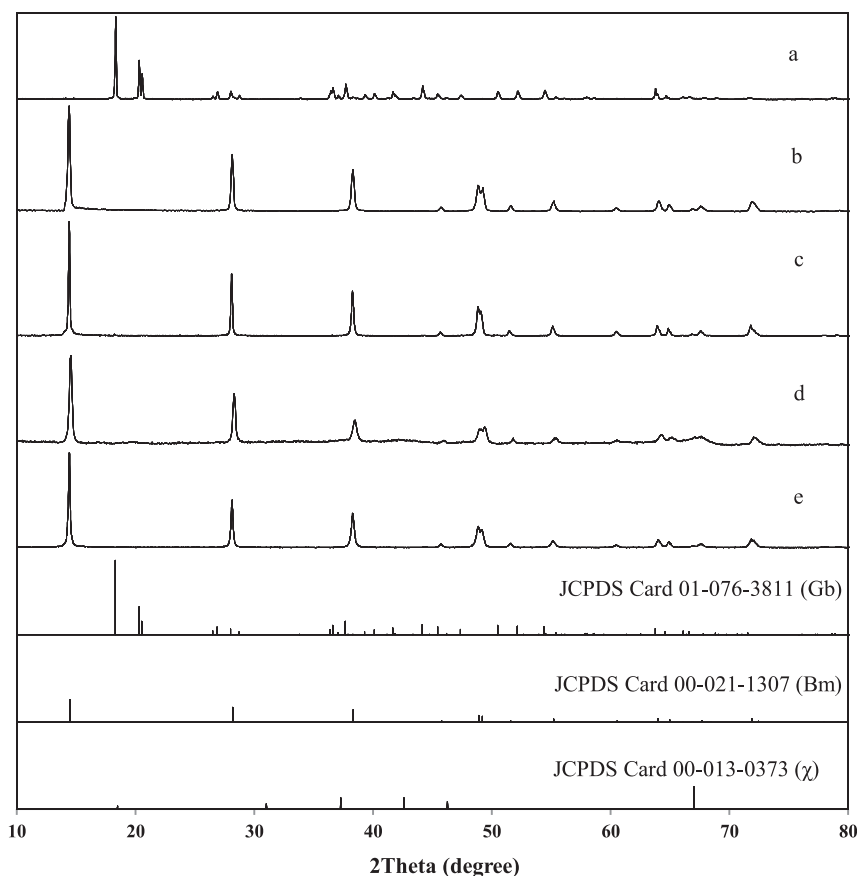

Fig. 2. XRD patterns of the product of the γ-Al(OH)$_3$ (a), the sample S1 (b), the sample S2 (c), the sample S3 (d), the sample S4 (e); Gb – gibbsite, Bm – boehmite, χ - χ-Al$_2$O$_3$.
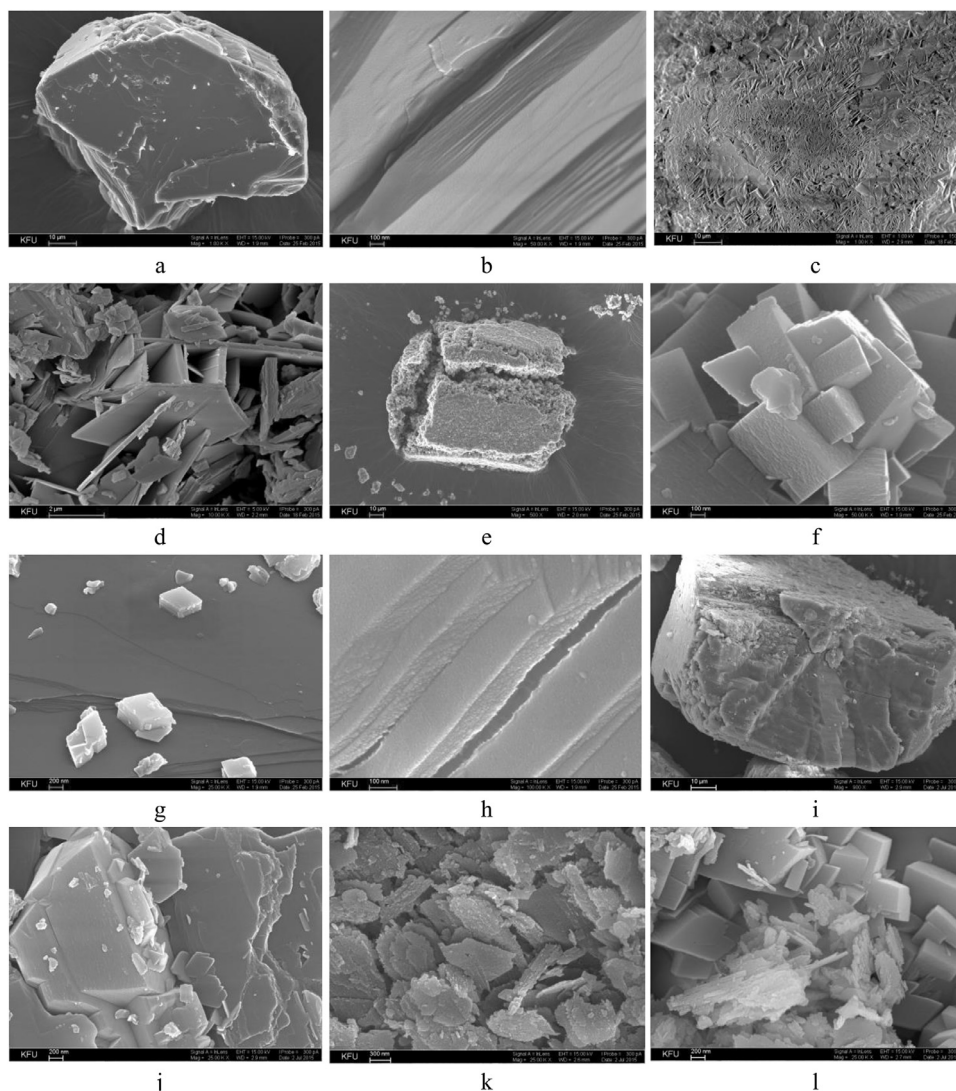
Fig. 3. SEM images of γ-Al(OH)$_3$ agglomerates chip (a), γ-Al(OH)$_3$ crystal crack (b), the sample S1 γ-AlOOH particles (c, d), the sample S2 γ-AlOOH particles and agglomerates chip (e, f), the sample S2 γ-AlOOH crystals on the γ-Al(OH)$_3$ crystal plates (g), γ-Al(OH)$_3$ crystal layers and slit between it (h), the sample S3 agglomerates outside (i) and inside (j) surfaces, the sample S4 agglomerates outside (k) and inside (l) surface.

crystals on Fig. 3f are equitable with the CSR sizes of γ-AlOOH and its sizes are 1.4–1.8 times larger than in the samples obtained under the "dry steam" conditions (Table 1).

The temperature minimum of the endothermic effect on the DSC curve of the dehydration reaction of γ-AlOOH to γ-Al$_2$O$_3$ is shifted to 558 °C due to the crystallization of the larger γ-AlOOH particles by dissolution-precipitation mechanism in the suspension. The purification of aluminum ions into the mother liquor suspension after the γ-Al(OH)$_3$ hydrothermal treatment is confirmed by ^{27}Al NMR analysis.

As shown on the Fig. 4a, b the ^{27}Al NMR spectrum of the mother liquor sample includes the signals with the chemical shift of 80.7 ppm which indicates the presence of mononuclear anions [Al(OH)$_4$]$^-$ [16] along, and with a signal with the chemical shift of 0.7 ppm indicating the aluminum cations in complexes [Al(H$_2$O)$_6$]$^{3+}$ in an aqueous solution of AlCl$_3$, which was used as an external mark.

Nucleus formation and γ-AlOOH 3D rhombus-shaped crystals growth (Fig. 3g) are carried out on γ-Al(OH)$_3$ plates surface, formed after flaking its crystal along the (001) plane. According to the SEM (Fig. 3h) the extended layers of γ-Al(OH)$_3$ crystals (the thick ~ 20–100 nm) arranged in parallel to each other with a crack between layers (the width ~ 10–50 nm) are identified in the samples which are obtained at $T = 180$ °C, $τ = 180$ min and pH = 10.5, after partial phase

transition (γ-AlOOH contain is ~ 22 wt.%).

In contrast to the processes described above the heat treatment mode that was chosen here under the atmospheric pressure provides complete dehydration γ-Al(OH)$_3$ to γ-AlOOH and χ-Al$_2$O$_3$ [15] without the agglomerates breaking (Fig. 1, curve 4). As shown on the Fig. 2d, the heat treatment product XRD pattern has the diffraction lines of both γ-AlOOH and χ-Al$_2$O$_3$. The phase transition temperature from γ-AlOOH to γ-Al$_2$O$_3$ is determined by the size of the hydroxide crystals: the more the hydroxide has particle size, the higher the temperature is [17]. So, dehydration of the obtained γ-AlOOH to γ-Al$_2$O$_3$ is characterized by two distinct endothermic effects with $T_{min} = 425$ °C and 544 °C (the first of which passes into the second) on the DSC curve of the sample, which we suggest belong to the fine and coarse crystalline γ-AlOOH formed particles respectively.

According to the SEM (Fig. 3i), the γ-Al(OH)$_3$ heat treatment product has smoothed outer surface of the crystals without cracks. As shown Fig. 2d the heat treatment products are γ-AlOOH and χ-Al$_2$O$_3$ (Table 1). The cut of agglomerate has nonporous 3D block particles islets in the form of parallelepipeds with a size from 0.3 to 1.5 μm and 2D particles in the form of plates, formed by close packing of smaller particles of the size ~ 20 nm around it (Fig. 3j).

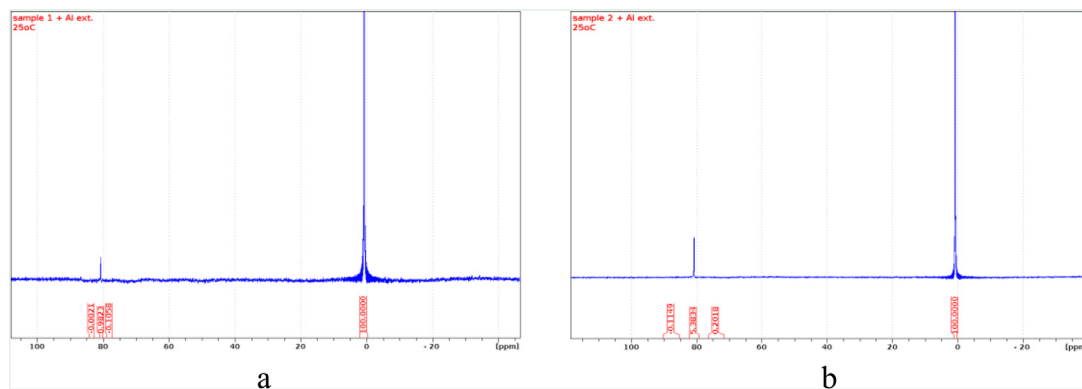Using the TEM data shown on Fig. 5a, we refer the former to γ-

Fig. 4. The NMR ^{27}Al spectrum of aluminum hydroxides mother liquor obtained by γ-Al(OH)$_3$ hydrothermal treatment of 200 °C, pH = 10.5 (the sample S2) during 30 min (a) and 60 min (b).

AlOOH parallelepiped-shaped particles with size of 50 to 500 nm.

The wide variation in the crystals size confirms the presence of a fine-grained and coarse γ-AlOOH. The smallest particles may be interpreted as primary γ-AlOOH particles since their sizes are consistent with the CSR sizes (Table 1). We can supposed that the particles are the

cause of the γ-AlOOH→γ-Al$_2$O$_3$ phase transition on the DSC curve at 425 °C. It is noted from TEM micrograph (Fig. 5b) that the structure of the crystals is nonporous [18,19]. As shown on the Fig. 5c a circular diffraction pattern has well-defined rings with the interplanar spacings of d_{hkl} = 0.235, 0.177, 0.166 nm, obtained from a site with a
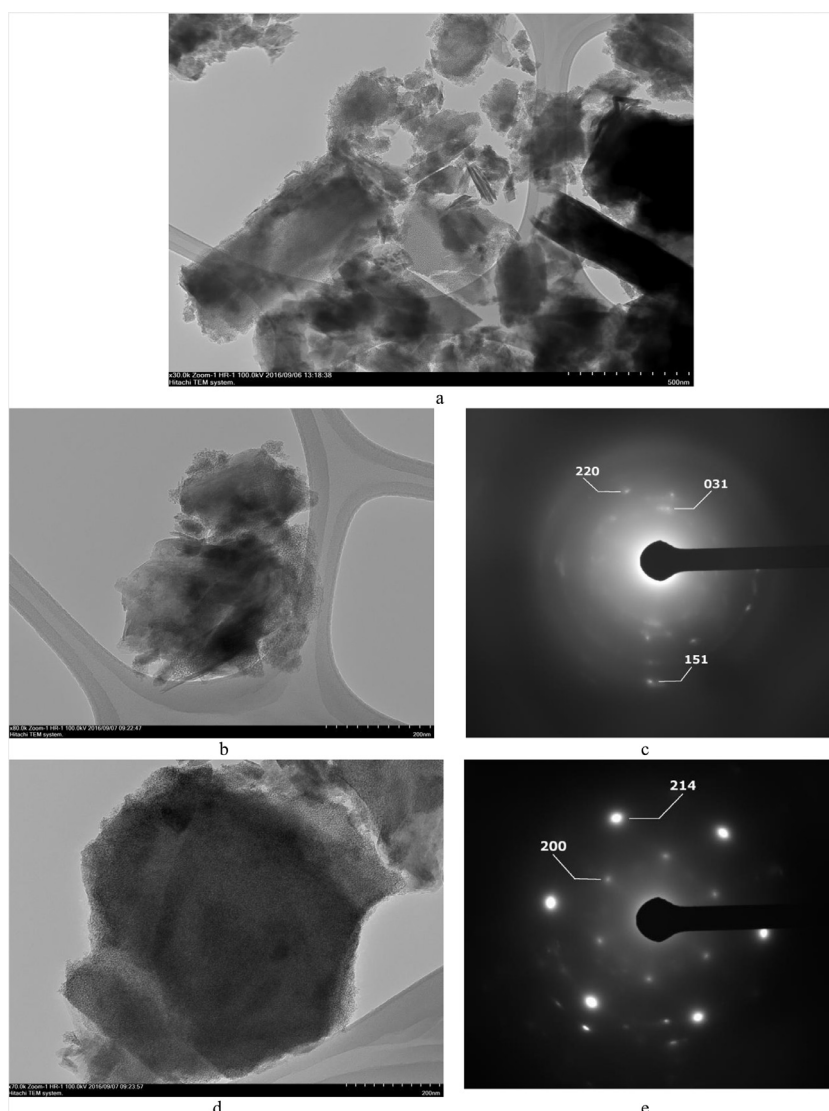

Fig. 5. TEM images of the sample S3: γ-AlOOH and χ-Al$_2$O$_3$ particles (a); (c) shows the corresponding SAED patterns of the γ-AlOOH particle shown in (b); (e) shows the corresponding SAED patterns of the χ-Al$_2$O$_3$ particle shown in (d).
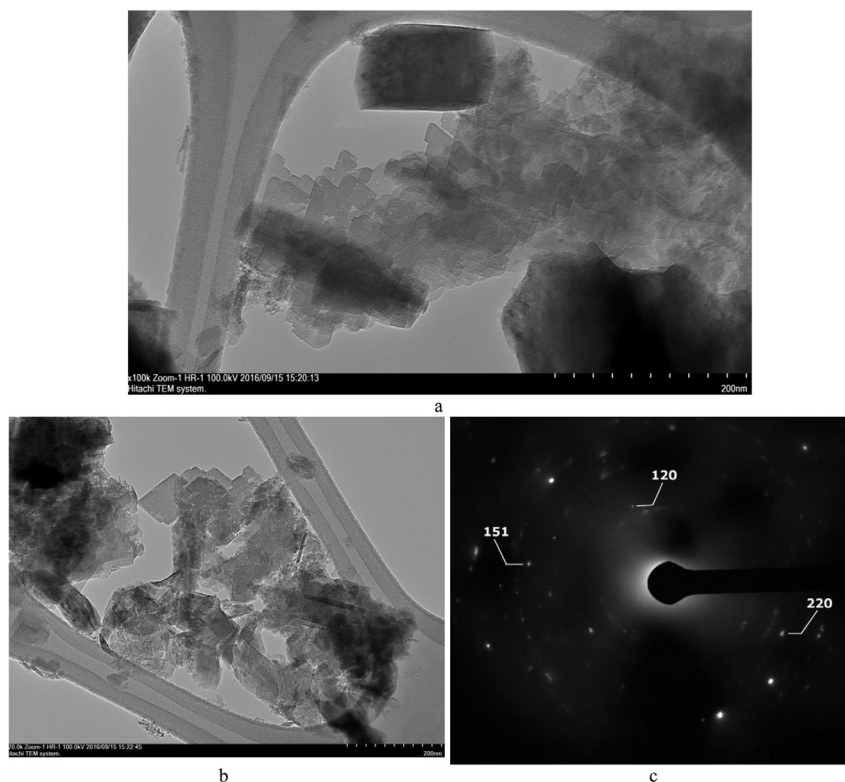
Fig. 6. TEM images of the sample S4: γ-AlOOH particles (a); (c) shows the corresponding SAED patterns of the γ-AlOOH particle shown in (b).

predominant content of 3D fragments, is typical for γ-AlOOH (JCPDS Card 00-021-1307) [20,21], in agreement with the XRD results (Fig. 2d).

We attribute the others 2D plate-shaped particles to the χ-Al₂O₃. As is seen on the TEM images (Fig. 5d) they have the form of thin films of highly irregular shape. As shown on the Fig. 5f the electron diffraction pattern with interplanar distances d_{hkl} = 0.241 and 0.140 nm obtained on a site with a primary content of these fragments is typical for the single-crystal χ-Al₂O₃ (JCPDS Card 00-013-0373) [22,23], in agreement with the XRD results (Fig. 2d). According to TEM the 2D χ-Al₂O₃ particles have ∼ the pore sizes of 5.2 nm and the average pore diameter in the sample is 3.5 nm (Table 1), which is in agreement with the low-temperature nitrogen adsorption results. The presence of fine pores is the reason for the large specific surface area and pore volume of this sample (Table 1). γ-AlOOH 3D cause the conservation of the agglomerates size and integrity after the heat treatment of γ-Al(OH)₃ due to the pseudomorphism phenomenon, when γ-AlOOH block structure inherits the size and shape of the initial γ-Al(OH)₃ particles and the majority of crystallization bonds between the particles forming the skeleton agglomerates remain unbroken.

Hydrothermal treatment of such phase mixture for 60 minutes at 200 °C provides the formation of almost monophasic γ-AlOOH (Fig. 2e; Table 1.) keeping the agglomerates size and integrity (Fig. 1, curve 5). A well-defined electron diffraction pattern could be obtained on the Fig. 6c and successfully assigned to the boehmite structure (JCPDS Card 00-021-1307), in agreement with the XRD results (Fig. 2e). The amount of coarse γ-AlOOH after the hydrothermal treatment is increased. The low-temperature endothermic effect of fine crystalline γ-AlOOH dehydration to γ-Al₂O₃ disappears on the DSC curve while the effect of dehydration coarse γ-AlOOH retains its position at T_{min} = 544 °C with an increase in weight loss. The number of coarse γ-AlOOH is increased by improvement of the structure of its fine crystalline (FC) phase and phase transition of χ-Al₂O₃ phase to coarse γ-AlOOH under hydrothermal treatment by the following scheme:

$$\gamma - AlOOH + FC\gamma - AlOOH + \chi - Al_2O_3 \rightarrow \gamma - AlOOH$$

This process increases the CSR size of γ-AlOOH of by approximately 1.3 times (Table 1).

According to the SEM on Fig. 3k, γ-AlOOH 2D particles are formed with a scale shape and a size of 50–500 μm, which in turn are formed by a dense rod-like fragments (thickness ∼ 10–50 μm).

As we see on the microphotograph TEM (Fig. 6a) γ-AlOOH 2D particles are formed by the layer packaging of the filmy lozenge-like crystals with an edge length of 10–20 nm.

Pores with an average diameter of 13 nm, volume of 0.1 cm³/g and the specific surface area of 29 m²/g, which is 9–22 times more than for γ-AlOOH samples obtained by γ-Al(OH)₃ hydrothermal treatment (Table 1), are formed by the packless arrangement of 2D scaly particles inside the agglomerates. Most likely the limited internal volume of the agglomerates which prevents the growth of 3D γ-AlOOH particles contributes to crystallization of 2D scaly particle. The γ-AlOOH particles are formed in the shape of lozenge and blocks with an edge length of ∼ 200–500 nm only on the outside of agglomerates in the absence of spatial restrictions (Fig. 3l).

5. Conclusions

The regulation of the hydrothermal treatment conditions of large γ-Al(OH)₃ agglomerates showed on the following scheme allows to synthesize γ-AlOOH crystals with different morphology and sizes both on the micro- and macro-levels, which is important in the synthesis of inorganic materials based on it.

Fully dispersed agglomerates of γ-AlOOH with 2D plate-like particles were obtained by the hydrothermal treatment of γ-Al(OH)₃ under the "dry steam" conditions. γ-AlOOH 3D particles in the form of blocks and lozenges are crystallized in an aqueous suspension inside the cracked agglomerates by the dissolution-precipitation mechanism.

Heat treatment of γ-Al(OH)₃ at atmospheric pressure causes the formation of micro- and macro-crystalline particles of γ-AlOOH in the form of blocks inside 3D particles which keep their integrity. After the

γ-Al(OH)$_3$ hydrothermal treatment of heat treatment product the three types of γ-AlOOH agglomerates were obtained. There are the 3D wireframe coarse γ-AlOOH particles in the form of blocks obtained at the heat treatment step along with the improve of the microcrystalline the structure, the 2D γ-AlOOH particles inside of agglomerates with the flake-shaped crystals formed by phase transition of χ-Al$_2$O$_3$, and 3D γ-AlOOH particles with the block- and lozenge-shaped crystals formed by phase transition χ-Al$_2$O$_3$ on the outside of the agglomerates.

Acknowledgments

References

[1] M.K. Naskar, M. Chatterjee, Boehmite nanoparticles by the two-reverse emulsion technique, J. Am. Ceram. Soc. 88 (2005) 3322–3326, https://doi.org/10.1111/j.1551-2916.2005.00600.x.

[2] Y. Feng, W. Lu, L. Zhang, X. Bao, B. Yue, Y. Iv, X. Shang, One-step synthesis of hierarchical cantaloupe-like AlOOH superstructures via a hydrothermal route, Cryst. Growth Design 8 (2008) 1426–1429, https://doi.org/10.1021/cg7007683.

[3] X. Wu, B. Zhang, Z. Hu, Morphology-controlled hydrothermal synthesis of boehmite via an anions competition method, Powder Technol. 239 (2013) 272–276, https://doi.org/10.1016/j.powtec.2013.02.023.

[4] Y. Li, J. Liu, Z. Jia, Fabrication of boehmite AlOOH nanofibers by a simple hydrothermal process, Mater. Lett. 60 (2006) 3586–3590, https://doi.org/10.1016/j.matlet.2006.03.083.

[5] G. Ji, M. Li, G. Li, G. Gao, H. Zou, S. Gan, X. Xu, Hydrothermal synthesis of hierarchical micron flower-like γ-AlOOH and γ-Al2O3 superstructures from oil shale ash, Powder Technol. 215–216 (2012) 54–58, https://doi.org/10.1016/j.powtec.2011.09.005.

[6] Y. Liu, D. Ma, X. Han, X. Bao, W. Frandsen, D. Wang, D. Su, Hydrothermal synthesis of microscale boehmite and gamma nanoleaves alumina, Mater. Lett. 62 (2008) 1297–1301, https://doi.org/10.1016/j.matlet.2007.08.067.

[7] M.G. Ma, Y.J. Zhu, Z.L. Xu, A new route to synthesis of γ-alumina nanorods, Mater. Lett. 61 (2007) 1812–1815, https://doi.org/10.1016/j.matlet.2006.07.138.

[8] Y. Zhao, R.L. Frost, W.N. Martens, H.Y. Zhu, Growth and surface properties of boehmite nanofibers and nanotubes at low temperatures using a hydrothermal synthesis route, Langmuir: ACS J. Surf. Colloids 23 (2007) 9850–9859, https://doi.org/10.1021/la700291d.

[9] M.W. Ross, T.C. DeVore, Desorption of nitric acid from boehmite and gibbsite, J. Phys. Chem. A 112 (2008) 6609–6620, https://doi.org/10.1021/jp7110555.

[10] Q. Zhang, S. Zhang, Y. Deng, Recent advances in ionic liquid catalysis, Green Chem. 13 (2011) 2619, https://doi.org/10.1039/c1gc15334j.

[11] S. Ram, S. Rana, Synthesis of mesoporous clusters of (AlO(OH)·αH2O) by a surface hydrolysis reaction of pure Al-metal with nascent-surface in water, Mater. Lett. 42 (2000) 52–60, https://doi.org/10.1016/S0167-577X(99)00158-5.

[12] P.K. Panda, V.A. Jaleel, S. Usha Devi, Hydrothermal synthesis of boehmite and α-alumina from Bayer's alumina trihydrate, J. Mater. Sci. (2006) 8386–8389, https://doi.org/10.1007/s10853-006-0771-7.

[13] C.J. Oh, Y.K. Yi, S.J. Kim, T. Tran, M.J. Kim, Production of micro-crystalline boehmite from hydrothermal processing of Bayer plant alumina tri-hydrate, Powder Technol. 235 (2013) 556–562, https://doi.org/10.1016/j.powtec.2012.10.041.

[14] T. Tsuchida, Hydrothermal synthesis of submicrometer crystals of boehmite, J. Eur. Ceram. Soc. 20 (2000) 1759–1764, https://doi.org/10.1016/S0955-2219(00)00052-2.

[15] K. Belaroui, M.N. Pons, H. Vivier, Morphological characterisation of gibbsite and alumina, Powder Technol. 127 (2002) 246–256, https://doi.org/10.1016/S0032-5910(02)00112-2.

[16] Y. Mathieu, S. Rigolet, V. Valtchev, B. Lebeau, Investigations of a sodium-poly-acrylate-containing system yielding nanosized boehmite particles, J. Phys. Chem. C 112 (2008) 18384–18392, https://doi.org/10.1021/jp806404e.

[17] F. Karouia, M. Boualleg, M. Digne, P. Alphonse, The impact of nanocrystallite size and shape on phase transformation: application to the boehmite/alumina transformation, Adv. Powder Technol. 27 (2016) 1814–1820, https://doi.org/10.1016/j.apt.2016.06.014.

[18] N. Nagai, Y. Suzuki, C. Sekikawa, T.Y. Nara, Y. Hakuta, T. Tsunoda, F. Mizukami, Fabrication of boehmite films with cage-like pores and their properties as enzyme immobilization supports, J. Mater. Chem. 22 (2012) 3234, https://doi.org/10.1039/c2jm15704g.

[19] C. Kaya, J.Y. He, X. Gu, E.G. Butler, Nanostructured ceramic powders by hydrothermal synthesis and their applications, Microporous Mesoporous Mater. 54 (2002) 37–49, https://doi.org/10.1016/S1387-1811(02)00334-7.

[20] R.W. Hicks, T.J. Pinnavaia, Nanoparticle assembly of mesoporous AlOOH (Boehmite), Chem. Mater. 15 (2003) 78–82, https://doi.org/10.1021/cm020753f.

[21] H. De Souza Santos, T.W. Campos, P. De Souza Santos, P.K. Kiyohara, Thermal phase sequences in gibbsite/kaolinite clay: electron microscopy studies, Ceram. Int. 31 (2005) 1077–1084, https://doi.org/10.1016/j.ceramint.2004.10.018.

[22] T. Kogure, Dehydration sequence of Gibbsite by electron-beam irradiation in a TEM, J. Am. Ceram. Soc. 82 (2004) 716–720, https://doi.org/10.1111/j.1151-2916.1999.tb01822.x.

[23] P.S. Santos, H.S. Santos, S.P. Toledo, Standard transition aluminas. Electron microscopy studies, Mater. Res. 3 (2000) 104–114, https://doi.org/10.1590/S1516-14392000000400003.